Frequency Domain Characteristics in Nonlinear Trimmer Dynamics

J. P. Harris [1]†, J. Mujica [2], V. Rottschäfer [3,4], and E. Sandin [2]

[1] *Mathematical Institute, University of Oxford, Oxford, UK*
[2] *Department of Mathematics, Vrije Universiteit Amsterdam, Amsterdam, The Netherlands*
[3] *Mathematical Institute, Leiden University, Leiden, The Netherlands*
[4] *Korteweg–de Vries Institute for Mathematics, University of Amsterdam, Amsterdam, The Netherlands*

(*Communicated to* MIIR *on 15 May 2024*)

Study Group: ESGI170, Study Group Mathematics with Industry, University of Groningen, 30 January – 03 February, 2023.
Communicated by: Julian Koellermeier, Pieter Tibboel, Stephan Trenn.
Industrial Partner: Philips.
Presenter: Daniel Driksz.
Team Members: J. P. Harris, Mathematical Institute, University of Oxford, Oxford, UK; J. Mujica, Department of Mathematics, Vrije Universiteit Amsterdam, Amsterdam, The Netherlands; V. Rottschäfer, Mathematical Institute, Leiden University, Leiden, The Netherlands, and Korteweg–de Vries Institute for Mathematics, University of Amsterdam, Amsterdam, The Netherlands; E. Sandin, Department of Mathematics, Vrije Universiteit Amsterdam, Amsterdam, The Netherlands.

Industrial Sector: Mechanics.

Key Words: Asymptotic analysis, coupled oscillators, nondimensionalisation.

MSC2020 Codes: 34E05, 70G60, 70K28.

Summary

We analyse a dynamical system describing the movement of the blade of a hair trimmer. Using nondimensionalisation and perturbation methods, we systematically analyse this model, with the goal of explaining a dip in the current amplitude observed in numerical simulations. We find that the motion of the blade is controlled by seven dimensionless parameters, and the dip in amplitude of the current corresponds to one of the dimensionless parameter groups taking the value of one. There is excellent agreement between our asymptotic solutions and long-time behaviour of the model revealed by numerical simulation.

† Corresponding Author: harris@maths.ox.ac.uk.

1 Introduction

At the Study Group Mathematics with Industry in Groningen in 2023, we worked on a problem posed by Philips. Philips manufacture, amongst many other products, hair and beard trimmers and their question was related to these. A picture of such a trimmer is given in Figure 1(a).

Philips use dynamical models to simulate and analyse the dynamic motion of the trimmer, in order to optimise performance. A simple but relevant model is one in which a dc-motor is coupled to a mass spring damper system (the cutting element). Individually, each system has linear dynamics. However, the interconnection between them is nonlinear which makes the whole system nonlinear.

The mechanical part of the shaver head consists of a toothed blade, attached via a small piece of plastic (the driving bridge) to an eccentric pin on a motor. The motion of the blade is restricted by two springs attached to the casing of the shaver head. The blade cuts hair which passes between itself and a comb mounted to the shaver head casing. A diagram of a shaver head is shown in Figure 1(b).

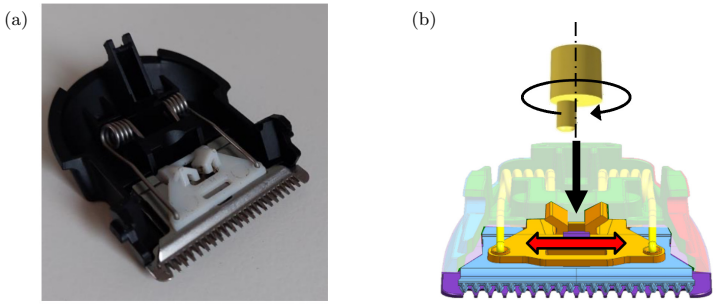

Figure 1. A typical trimmer head (a) and a schematic representation of its functioning (b). Figures provided by Philips.

The model we analyse is described by equations (2.1)–(2.4) with typical parameter values given in Table 1. The motor current through the electric part consists of a dc-component and a sinusoidal component. When performing numerical simulations, Philips observed that when varying the voltage $\hat{V}$, the amplitude of the sinusoidal part of the motor current attains a minimum for a certain value of $\hat{V}$. See Figure 2 for the results of a numerical simulation where parameter values are taken as in Table 1 for two different choices of one of the parameters, $\hat{k}_s$. Philips would like to know whether this point can be determined using analytical methods. We provide insight in this behaviour using the techniques of nondimensionalisation and asymptotic analysis. These methods are widely applicable and can also be used for other (larger) systems.

First, in Section 2, we formulate the model, introduce the concept of nondimensionalisation and make the system dimensionless. Then, in Section 3, we use asymptotic analysis to study the solutions to the dimensionless system. Finally, in Section 4, we conclude with a discussion and recommendations.

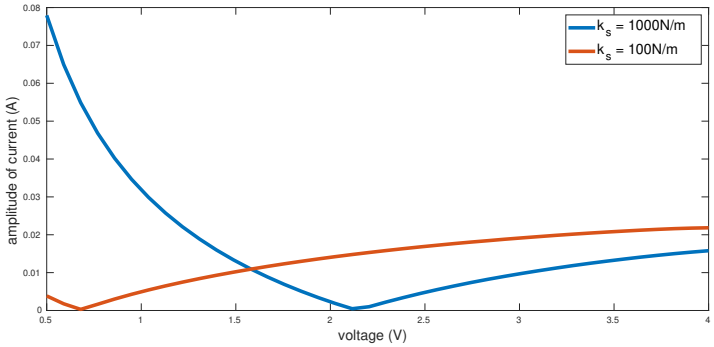

Figure 2. The amplitude of the oscillatory part of the motor current as a function of voltage from numerical solution of (2.1)–(2.3) for $\hat{k}_s = 1000N/m$ (blue) and $\hat{k}_s = 100N/m$ (red). All other parameters are taken from Table 1.

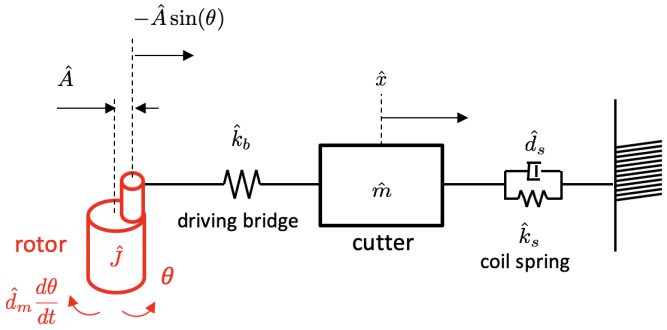

Figure 3. Physical set up for the coupled system (2.1)–(2.4).

2 Model

We study a physical model of the shaver head. The model is illustrated in Figure 3. We model the shaver head casing as a rigid wall, to which the blade is connected via a linearly-damped Hookean spring with spring constant $\hat{k}_s$, and damping coefficient $\hat{d}_s$. The blade, of mass $\hat{m}$, is attached to the eccentric pin of the motor via the driving bridge which we model as a Hookean spring with stiffness $\hat{k}_b$. We assume that the driving bridge is connected to the motor pin at all times, and slides without friction in such a way that the blade moves only in one line, radially from the centre of the motor. We denote the displacement of the blade, at time $\hat{t}$, by $\hat{x}(\hat{t})$. We assume the motor centre is fixed relative to the shaver head casing, and we denote the distance between the centre of the motor and the eccentric pin by $\hat{A}$. We denote the angle of the pin from its starting position by $\theta(\hat{t})$. We assume the motor has inertia $\hat{J}$, self-inductance $\hat{L}$, resistance $\hat{R}$, motor constant $\hat{K}$, and a linear damping coefficient of $\hat{d}_m$. We denote the current through the motor by $\hat{I}(\hat{t})$. We assume the system is at rest before a constant voltage, $\hat{V}$, is applied across the motor for times $\hat{t} > 0$. Typical values for each of the parameters are given in Table 1.

Using the principles of conservation of momentum, angular momentum and (electrical)

https://doi.org/10.33774/miir-2024-cj024

$\hat{m}$	$\hat{k}_s$	$\hat{d}_s$	$\hat{k}_b$	$\hat{A}$	$\hat{J}$
kg	kg s^{-2}	kg m s^{-1}	kg s^{-2}	m	kg m^2
$3.5 \cdot 10^{-3}$	10^3	0.025	$4 \cdot 10^3$	$1.5 \cdot 10^{-3}$	$3 \cdot 10^{-7}$
$\hat{K}$	$\hat{d}_m$	$\hat{L}$	$\hat{R}$	$\hat{V}$	
kg m^2 A^{-1} s^{-2}	kg m s^{-1}	kg m^2 s^{-2} A^{-2}	V A^{-1}	V	
$4 \cdot 10^{-3}$	0	$0.5 \cdot 10^{-3}$	0.7	1	

Table 1. Model parameters and their units, together with typical values provided by Philips.

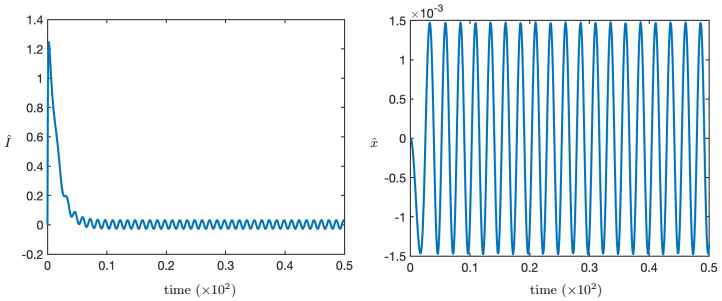

Figure 4. Solution to (2.1)–(2.4), with parameters values taken from Table 1. Shown are time series for $\hat{I}$ (left) and $\hat{x}$ (right). Note that after a short transient, the current of the motor stabilizes following periodic motion.

energy, we write down a system of three coupled ODEs for $\hat{x}, \theta, \hat{I}$,

$$\hat{m}\frac{\mathrm{d}^2\hat{x}}{\mathrm{d}\hat{t}^2} = -\hat{k}_s\hat{x} - \hat{d}_s\frac{\mathrm{d}\hat{x}}{\mathrm{d}\hat{t}} - \hat{k}_b\left(\hat{x} + \hat{A}\sin(\theta)\right), \tag{2.1}$$

$$\hat{J}\frac{\mathrm{d}^2\theta}{\mathrm{d}\hat{t}^2} = \hat{K}\hat{I} - \hat{d}_m\frac{\mathrm{d}\theta}{\mathrm{d}\hat{t}} - \hat{k}_b\hat{A}\cos(\theta)\left(\hat{x} + \hat{A}\sin(\theta)\right), \tag{2.2}$$

$$\hat{L}\frac{\mathrm{d}\hat{I}}{\mathrm{d}\hat{t}} = -\hat{K}\frac{\mathrm{d}\theta}{\mathrm{d}\hat{t}} - \hat{R}\hat{I} + \hat{V}. \tag{2.3}$$

To specify a particular solution of this model, we impose five initial conditions,

$$\hat{x} = \frac{\mathrm{d}\hat{x}}{\mathrm{d}\hat{t}} = \theta = \frac{\mathrm{d}\theta}{\mathrm{d}\hat{t}} = \hat{I} = 0, \quad \text{at} \quad \hat{t} = 0, \tag{2.4}$$

corresponding to the system initially being at rest.

The model described by equations (2.1)–(2.4) is well-posed, and is readily solved numerically using off-the-shelf ODE solvers, such as MATLAB `ode45`. A numerical solution to (2.1)–(2.4) for the parameter values in Table 1 is shown in Figure 4.

To investigate the behaviour of this model, we *could* use a numerical approach such as repeated integration of the full coupled second-order system while sweeping through different values of the dimensional parameters or try to use a numerical continuation approach of the equivalent first-order vector field representation of the model. However, we are able to reduce the size of the parameter space by first *nondimensionalising*.

2.1 Nondimensionalisation

When faced with a model such as (2.1)–(2.4), there are a number of benefits to rescaling the variables to remove their dimensions:

- We are able to identify dimensionless groups of parameters which control the behaviour of the model, reducing the size of the parameter space.
- It does not make sense to compare quantities with different dimensions; who is to say a kilogram is small compared to a metre when they are fundamentally different quantities? By removing dimensions we are able to compare the size of different terms in a model, which may allow us to identify which processes are dominating the behaviour of the model.
- The size of the dimensionless variables can be chosen so they are not too large or too small, meaning that the dimensionless version of the model is often less susceptible than the dimensional model to stability issues when solving numerically.

The dimensionless model captures exactly the same physics as the dimensional model, and we can always rescale the solutions to the dimensionless model to put them back in dimensional terms.

We will present how to nondimensionalise the model described by equations (2.1)–(2.4) in enough detail to understand how to nondimensionalise other similar models. Note that some of the choices we make along the way are not unique. However, if we had made alternative choices we would still find that that set of dimensionless parameters is similar to those we derive here. The technique of nondimensionalisation is a useful first step in evaluating any physical mathematical model. More examples and discussion of nondimensionalisation are given in [5, §1], where it is referred to as normalization, and in [1].

To start with, we rescale each of the *dimensional* variables, denoted with hats, with a typical *dimensional* scale, which we denote by square brackets, as so:

$$\hat{x} = [x]x, \quad \hat{I} = [I]I, \quad \hat{t} = [t]t. \tag{2.5}$$

The variables x, I and θ are *dimensionless* dependent variables, and t is the *dimensionless* independent variable. Note that θ denotes an angle measured in radians, so it is already dimensionless. At this stage, we are free to choose the dimensional scalings, $[x]$, $[I]$ and $[t]$. We may have an idea of what sensible scalings could be from experiments or numerical simulations, but for now, we leave them as unknown constants. We will choose them later to simplify the model as much as we can.

Substituting (2.5) into the governing equations[1] (2.1)–(2.3) we find

$$\frac{\hat{m}[x]}{[t]^2}\frac{\mathrm{d}^2x}{\mathrm{d}t^2} = -\hat{k}_s[x]x - \frac{\hat{d}_s[x]}{[t]}\frac{\mathrm{d}x}{\mathrm{d}t} - \hat{k}_b\left([x]x + \hat{A}\sin(\theta)\right), \tag{2.6}$$

$$\frac{\hat{J}}{[t]^2}\frac{\mathrm{d}^2\theta}{\mathrm{d}t^2} = \hat{K}[I]I - \frac{\hat{d}_m}{[t]}\frac{\mathrm{d}\theta}{\mathrm{d}t} - \hat{k}_b\hat{A}\cos(\theta)\left([x]x + \hat{A}\sin(\theta)\right), \tag{2.7}$$

$$\frac{\hat{L}[I]}{[t]}\frac{\mathrm{d}I}{\mathrm{d}t} = -\frac{\hat{K}}{[t]}\frac{\mathrm{d}\theta}{\mathrm{d}t} - \hat{R}[I]I + \hat{V}. \tag{2.8}$$

To make these equations dimensionless we divide through each of the equations so one of the terms is dimensionless (has no hats or square brackets). It does not really matter how we choose to do this, but one possibility is

$$\frac{\hat{m}}{\hat{k}_s[t]^2}\frac{\mathrm{d}^2x}{\mathrm{d}t^2} = -x - \frac{\hat{d}_s}{\hat{k}_s[t]}\frac{\mathrm{d}x}{\mathrm{d}t} - \frac{\hat{k}_b}{\hat{k}_s}\left(x + \frac{\hat{A}}{[x]}\sin(\theta)\right), \tag{2.9}$$

$$\frac{\mathrm{d}^2\theta}{\mathrm{d}t^2} = \frac{\hat{K}[I][t]^2}{\hat{J}}I - \frac{\hat{d}_m[t]}{\hat{J}}\frac{\mathrm{d}\theta}{\mathrm{d}t} - \frac{\hat{k}_b\hat{A}[x][t]^2}{\hat{J}}\cos(\theta)\left(x + \frac{\hat{A}}{[x]}\sin(\theta)\right), \tag{2.10}$$

$$\frac{\hat{L}[I]}{\hat{V}[t]}\frac{\mathrm{d}I}{\mathrm{d}t} = -\frac{\hat{K}}{\hat{V}[t]}\frac{\mathrm{d}\theta}{\mathrm{d}t} - \frac{\hat{R}[I]}{\hat{V}}I + 1. \tag{2.11}$$

Finally, because we are still free to choose $[x]$, $[I]$ and $[t]$, we are able to set three further coefficients in (2.9)–(2.11) to be equal to one, reducing the number of parameters. Again, it does not really matter which terms we choose, but if we have some physical insight into the system this can be helpful. For instance, one could imagine that the amplitude of displacement of the mass might be similar to the radial distance, $\hat{A}$, between the centre of the motor and the eccentric pin. In which case, it would be sensible to set $\hat{A}/[x] = 1$. We further choose the time-scale to balance the acceleration of the blade with the force due to the spring, and choose the current-scale to balance the voltage and resistance, so that our dimensional scalings are

$$[x] = \hat{A}, \quad [I] = \frac{\hat{V}}{\hat{R}}, \quad [t] = \sqrt{\frac{\hat{m}}{\hat{k}_s}}. \tag{2.12}$$

The resulting dimensionless model is

$$\frac{\mathrm{d}^2x}{\mathrm{d}t^2} = -x - d_s\frac{\mathrm{d}x}{\mathrm{d}t} - \lambda(x + \sin\theta), \tag{2.13}$$

$$\frac{\mathrm{d}^2\theta}{\mathrm{d}t^2} = \alpha K I - d_m\frac{\mathrm{d}\theta}{\mathrm{d}t} - \lambda\mu\cos\theta(x + \sin\theta), \tag{2.14}$$

$$L\frac{\mathrm{d}I}{\mathrm{d}t} = -K\frac{\mathrm{d}\theta}{\mathrm{d}t} - I + 1, \tag{2.15}$$

where the dimensionless parameters are defined in terms of the dimensional parameters in Table 2. The dimensionless initial conditions are

[1] In general, the initial conditions should be considered as part of the nondimensionalisation process. In this case, since the initial conditions (2.4) are homogeneous, rescaling the variables does not result in any additional dimensionless parameter groups.

d_s	λ	α	K	μ	L	d_m
$\frac{\hat{d}_s}{\sqrt{\hat{k}_s \hat{m}}}$	$\frac{\hat{k}_b}{\hat{k}_s}$	$\frac{\sqrt{\hat{m}^3}\hat{V}^2}{\sqrt{\hat{k}_s^3}\hat{R}\hat{J}}$	$\frac{\hat{K}\sqrt{\hat{k}_s}}{\hat{V}\sqrt{\hat{m}}}$	$\frac{\hat{m}\hat{A}^2}{\hat{J}}$	$\frac{\hat{L}\sqrt{\hat{k}_s}}{\hat{R}\sqrt{\hat{m}}}$	$\frac{\hat{d}_m\sqrt{\hat{m}}}{\hat{J}\hat{k}_s}$
$1.3 \cdot 10^{-2}$	40	$3.1 \cdot 10^{-2}$	2.1	$2.9 \cdot 10^{-2}$	0.38	0

Table 2. Definitions of the dimensionless parameters, and typical values based on the values in Table 1.

$$x = \frac{\mathrm{d}x}{\mathrm{d}t} = \theta = \frac{\mathrm{d}\theta}{\mathrm{d}t} = I = 0, \quad \text{at} \quad t = 0. \tag{2.16}$$

Based on the typical values provided in Table 1, the dimensional scalings (2.12) are approximately $[x] = 1.5 \times 10^{-3}\,\mathrm{m}$, $[I] = 1.4\,\mathrm{A}$ and $[t] = 1.9 \times 10^{-3}\,\mathrm{s}$.

3 Asymptotic analysis

A number of the dimensionless parameters in Table 2 are small. There is a suite of mathematical techniques, called *perturbation methods*, used for finding approximate solutions to mathematical models with small parameters. The resulting solutions are *asymptotic approximations* to the solution. We will not precisely define what this means here, rather referring the reader to [2, §1–2] and [3].

The typical values for $\lambda^{-1}, d_s, \alpha, \mu$ in Table 2 are of a similar size, and all much less than one. We therefore seek a solution valid in the limit $\lambda \to \infty$ and $d_s, \alpha, \mu \to 0$, such that

$$\lambda\psi = O(1) \quad \text{as} \quad \lambda \to \infty, \tag{3.1}$$

where $\psi = d_s, \alpha, \mu$, hence, $\lambda^{-1}, d_s, \alpha$ and μ are all of the same order. Furthermore, we will assume that $d_m \equiv 0$ from here on in.

Formally, we seek a solution in the form

$$x \sim x_0 + \alpha x_1 + \cdots, \tag{3.2a}$$
$$\theta \sim \theta_0 + \alpha\theta_1 + \cdots, \tag{3.2b}$$
$$I \sim I_0 + \alpha I_1 + \cdots. \tag{3.2c}$$

The expressions (3.2) are asymptotic series. The key here is that each term is asymptotically smaller than the previous. For example, in (3.2a) we insist that $\alpha x_1/x_0 \to 0$ as we take the limit (3.1).

Substituting (3.2) into (2.13)–(2.15) and collecting the leading order terms, the equations are

$$x_0 + \sin(\theta_0) = 0, \tag{3.3}$$
$$\frac{\mathrm{d}^2\theta_0}{\mathrm{d}t^2} = 0, \tag{3.4}$$
$$L\frac{\mathrm{d}I_0}{\mathrm{d}t} = -K\frac{\mathrm{d}\theta_0}{\mathrm{d}t} - I_0 + 1. \tag{3.5}$$

The general solution to these differential equations is

$$x_0 = \sin(c_1 + \omega t), \tag{3.6}$$

$$\theta_0 = c_1 + \omega t, \tag{3.7}$$

$$I_0 = c_2 \exp\left(-\frac{t}{L}\right) + 1 - K\omega, \tag{3.8}$$

where ω, c_1, c_2 are constants to be determined. Unfortunately, if we try to apply the initial conditions (2.16), we find that ω, c_1, c_2 are all identically zero. This tells us that the balances we have chosen by assuming (2.12) are not the dominant balances during the initial motion of the blade.

We did not address this early time behaviour during the study group. Instead, we determined ω assuming that the scalings we have chosen represent the longer time behaviour of the system, assuming c_1, c_2 would come from analysing the, as yet unknown, early time behaviour.

To find the frequency, ω, we must consider the second order approximation,

$$\frac{\mathrm{d}^2 x_0}{\mathrm{d}t^2} = -x_0 - d_s \frac{\mathrm{d}x_0}{\mathrm{d}t} - \alpha\lambda(x_1 + \theta_1 \cos(\theta_0)), \tag{3.9}$$

$$\frac{\mathrm{d}^2 \theta_1}{\mathrm{d}t^2} = KI_0 - \lambda\mu \cos(\theta_0)(x_1 + \theta_1 \cos(\theta_0)), \tag{3.10}$$

$$L\frac{\mathrm{d}I_1}{\mathrm{d}t} = -K\frac{\mathrm{d}\theta_1}{\mathrm{d}t} - I_1. \tag{3.11}$$

These equations describe the balance between the largest terms in the limit (3.1) which we neglected in deriving (3.3)–(3.5)[2]. We can eliminate x_1 from (3.10) using (3.9) to find

$$\frac{\mathrm{d}^2 \theta_1}{\mathrm{d}t^2} = KI_0 + \frac{\mu}{\alpha}\cos(\theta_0)\left(\frac{\mathrm{d}^2 x_0}{\mathrm{d}t^2} + x_0 + d_s\frac{\mathrm{d}x_0}{\mathrm{d}t}\right). \tag{3.12}$$

Substituting the leading order solutions (3.6)–(3.8) into (3.12) we find

$$\begin{aligned}\frac{\mathrm{d}^2 \theta_1}{\mathrm{d}t^2} = K\left(c_2 \exp\left(-\frac{t}{L}\right) + 1 - K\omega\right) \\ - \frac{\mu}{\alpha}(1-\omega^2)\sin(c_1+\omega t)\cos(c_1+\omega t) \\ - \frac{\mu}{\alpha} d_s \omega \cos^2(c_1+\omega t).\end{aligned} \tag{3.13}$$

Integrating twice, we deduce

$$\begin{aligned}\theta_1 = Kc_2L^2 \exp\left(-\frac{t}{L}\right) + t^2\left(\frac{K(1-K\omega)}{2} - d_s\frac{\mu\omega}{4\alpha}\right) \\ + t\left(c_3 - \frac{\mu}{4\alpha\omega}\left(1-\omega^2\right)\right) + \frac{\mu}{8\alpha\omega^2}\left(1-\omega^2\right)\sin(2\theta_0) \\ + d_s\frac{\mu}{8\alpha\omega^2}\cos(2\theta_0) + c_4.\end{aligned} \tag{3.14}$$

where c_3, c_4 are constants of integration.

[2] It would be consistent with our asymptotic assumptions (3.1) to leave the $d_s \mathrm{d}x_0/\mathrm{d}t$ term out of equation (3.9). However, leaving it in does not make the system of equations more difficult to solve, and means our analysis is valid for $d_s = O(1)$.

For our asymptotic solution (3.2b) to be valid for large t, the perturbation, θ_1, can not grow faster than θ_0. In particular, this means that the coefficient of the quadratic term must be zero[3], so ω must satisfy

$$\frac{K(1-K\omega)}{2} - d_s\frac{\mu\omega}{4\alpha} = 0. \tag{3.15}$$

Hence,

$$\omega = \frac{2K}{2K^2 + d_s\mu/\alpha}. \tag{3.16}$$

As $d_s\mu/\alpha \to 0$, which is consistent with (3.1), we find that approximately

$$\omega \sim \frac{1}{K}. \tag{3.17}$$

Recall that for certain voltages Philips observed that the amplitude of the oscillatory part of the current drops to close to zero. To understand this phenomenon, we solve for the second order correction, I_1, to the current. We solve (3.11) using variation of parameters, seeking a solution of the form $I_1 = C(t)\exp(-t/L)$. The equation for $C(t)$ is

$$\frac{\mathrm{d}C}{\mathrm{d}t} = -\frac{K}{L}\exp\left(\frac{t}{L}\right)\frac{\mathrm{d}\theta_1}{\mathrm{d}t}. \tag{3.18}$$

Differentiating (3.14), and integrating (3.18), we find

$$\begin{aligned} C = c_5 + K^2c_2t - K\left(c_3 - \frac{\mu}{4\alpha\omega}\left(1-\omega^2\right)\right)\exp\left(\frac{t}{L}\right) \\ + \frac{K\mu\exp(t/L)}{4\alpha\omega\left(1+4L^2\omega^2\right)}\Bigg[\left(d_s - 2\omega L(1-\omega^2)\right)\sin(2\theta_0) \\ - \left(1-\omega^2+2\omega Ld_s\right)\cos(2\theta_0)\Bigg], \end{aligned} \tag{3.19}$$

where c_5 is a constant of integration. Therefore the correction to the current is

$$\begin{aligned} I_1 = \exp\left(-\frac{t}{L}\right)\left(c_5 + K^2c_2t\right) - K\left(c_3 - \frac{\mu}{4\alpha\omega}\left(1-\omega^2\right)\right) \\ + \frac{K\mu}{4\alpha\omega\left(1+4L^2\omega^2\right)}\Bigg[\left(d_s - 2\omega L(1-\omega^2)\right)\sin(2\theta_0) \\ - \left(1-\omega^2+2\omega Ld_s\right)\cos(2\theta_0)\Bigg]. \end{aligned} \tag{3.20}$$

The oscillatory part of I_1 is written in square brackets.

From our analysis, parameter d_s is $O(\alpha)$ in the limit (3.1). If also $1-\omega^2 = O(\alpha)$, then the amplitude of the oscillatory part of I_1 in (3.20) is $O(\alpha)$ as well. Considering the asymptotic expansion of the current, $I \sim I_0 + \alpha I_1 + \cdots$, this implies that the oscillatory part of the current is $O(\alpha^2)$. Therefore, we find the dip in current observed by Philips

[3] This implies that there exist multiple timescales in the problem. There are methods to analyse problems with multiple timescales, see [3, §3].

https://doi.org/10.33774/miir-2024-cj024

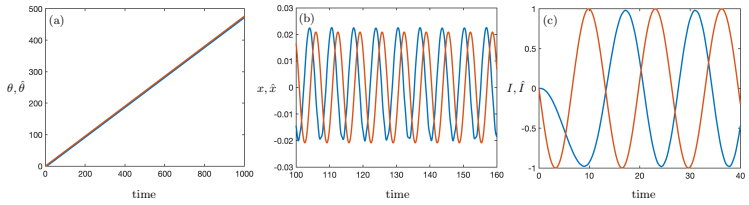

Figure 5. Comparison between numeric (blue) and leading-order dimensionless (red) solutions. Panels (a), (b) and (c) show time series of the angle, the displacement of the blade and the current through the motor, respectively.

occurs when ω is approximately one, which, from (3.17), we conclude occurs when K is also approximately one. Looking at the definition of K in Table 2, we see that the current drops when

$$\frac{\hat{K}\sqrt{\hat{k}_s}}{\hat{V}\sqrt{\hat{m}}} \approx 1. \tag{3.21}$$

Physically this means that the natural rotational speed of the motor matches the natural frequency of the spring-blade system. If there was no damping, $d_s = 0$, then the motor would approach a steady speed where it would not need to do work to keep the blade in motion.

4 Discussion and recommendations

We investigated a model for the dynamic motion of a trimmer proposed by Philips in order to understand and optimize its performance. The model is based on a classical mass-spring system and can be interpreted as two oscillators that are nonlinearly coupled.

Our approach is based on nondimensionalisation of the model, which reduces the number of parameters for further analysis. Some of the dimensionless parameters in the nondimensionalised system are small, and therefore, we use the methods of asymptotic analysis and look for asymptotic approximations to solutions of the system. This way we find explicit leading-order representations for the (dimensionless) displacement of the blade, x, the angle of the pin, θ, and the current through the motor, I, which show excellent agreement with the numerical simulation of the system described by equations (2.1)–(2.4). A comparison between the numerical solutions (blue) and the (dimensional) asymptotic solutions (red) is displayed in Figure 5. Panel (a) shows the long-term concordance of the angle of the pin, while panels (b) and (c) show agreement of the displacement and the current. Despite being slightly out of phase due to the choice of initial conditions, both solutions behave in the same way and within the same order of magnitude.

The trimmer dynamics model studied here provides interesting synchronization properties between two nonlinearly coupled oscillators. Nondimensionalisation together with asymptotic analysis has proven to be a useful tool to simplify the system and obtain a mathematical explanation for the dip in the motor current observed in simulations. Our recommendation is to use this approach in more extended versions of the given model, as it provides an organized way to obtain insights on the behaviour of relevant quantities. Alternatively, one could combine this analytic approach with a systematic numerical in-

vestigation of the reduced dimensionless parameter space, using, for instance, state of the art methods based on the numerical continuation of periodic solutions to the system under consideration; see, for instance, [4]. Though it would be worth exploring that path, we do not pursue that method in this report.

5 Acknowledgements

The authors would like to thank the organisers of SWI 2023, particularly Stephan Trenn, for all their hard work to make the study group a success. They would also like to thank Daniel Dirksz of Philips for presenting this interesting problem at the study group. J.P.H. acknowledges the support provided by the Engineering and Physical Sciences Research Council (EPSRC) Centre for Doctoral Training in Industrially Focused Mathematical Modelling (EP/L015803/1). J.M. acknowledges support from the EPSRC through the grant EP/T013613/1.

References

[1] J. W. Haefner. *Modeling Biological Systems*. Springer, 2005.
[2] E. J. Hinch. *Perturbation Methods*. Cambridge University Press, 1991.
[3] H. H. Holmes. *Introduction to Perturbation Methods*. Springer, 2013.
[4] B. Krauskopf, H. M. Osinga, and J. Galán-Vioque (eds). *Numerical Continuation Methods for Dynamical Systems: Path following and boundary value problems*. Springer Netherlands, 2007.
[5] A. B. Tayler. *Mathematical Models in Applied Mathematics*. Oxford University Press, 1986.